Comparison between Different Control Strategies of a Z-Source Inverter Based Dynamic Voltage Restorer

Abolfazl KAZEMDEHDASHTII[1], Ali Reza SEIFI[1], Amin Shabanpour HAGHIGHI[1]

[1]Department of Power and Control, Faculty of Electrical and Computer Engineering, Shiraz University, Zand Street, 71345 Shiraz, Iran

abolfazlkd@yahoo.com, seifi@shirazu.ac.ir, shabanpour.amin@gmail.com

Abstract. *In this paper, dynamic voltage restorer (DVR) compensation methods are compared to each other for the load side connected shunt converter topology of z-source inverter based DVR to choose the best method. Four different topologies are recognized for DVR that two of them have energy storage devices, and two topologies have no energy storage that take energy from the grid during the period of compensation. Here the load side connected shunt converter topology that takes necessary energy from the grid is used. Pre-sag compensation, in-phase compensation, energy-optimized methods are the three DVR compensation methods that studied and compared. A deep analysis through different diagrams would show the advantages or disadvantages of each compensation method. Equations for all methods are derived and the characteristics of algorithms are compared with each other. The simulation results done by SIMULINK/ MATLAB shows compensating by this topology based on the compensation methods.*

Keywords

Compensation methods, close loop control, dynamic voltage restorer, topology, Z-source inverter.

1. Introduction

Power quality has obtained more attention in recent years due to growth in using industrial sensitive loads [1]. Voltage sag is one of the most important power quality issues that occur in the shape of sudden voltage fall, which happens greatly due to short circuit fault. There are several solutions to this problem [2] and DVR is the most effective of them (for load voltage control and compensation). DVR consists of a converter, energy storage device and a transformer to inject the appropriate voltage to clear the power quality problems. The compensation ability of the conventional DVR (consists of the voltage source inverter) depends on the maximum value of energy storage. Due to the limitation of energy storage, a DC-DC boost converter is needed to use with VSI. In this paper, Z-source inverter, based DVR topology is used that has several advantages regarding cost, reliability and simplicity. In this topology, VSI and DC-DC boost converter is replaced by Z-source inverter [3]. Boosting the ability of Z-source inverter is about a switching state called shoot-through that is created by turning on both upper and lower switches of one phase [4], [5], [6] which is very important in reliability. Shoot-through is a unique switching state of Z-source inverter that is an unallowable state for conventional inverters that causes several disturbances [7].

Based on the type of energy storage, four different topologies of DVR are proposed. Two topologies can be realized with a minimum amount of energy storage that take energy from the grid during the compensation period and other topologies, take energy from internal energy storage devices [8]. Load side connected shunt converter topology of z-source inverter based DVR and the control method [9], [10] are discussed in section 2.

There are three compensation strategies for conventional DVR in literatures [11], [12]. Comparisons between them are done in for a general type of DVR. All compensation methods include pre-fault, in-phase, and energy optimized compensation algorithm are analyzed and compared in this paper for the Z-source inverter based DVR. Equations for each method are derived. Furthermore some parameters to characterize the behavior of each method for this special kind of DVR are defined. Finally, comparisons are done in various aspects to show the characteristics of each compensating algorithms.

In section 3 three compensation methods are discussed for the topology of the shunt converter connected to the load side of the z-source inverter based DVR and the equation helps to compare these compensation methods and choose one of them to show the operation of this topology to clear the power quality problem.

2. Proposed Topologies for Z-Source Inverter based DVR

Different topologies of DVR are applied in two parts. One uses energy storage to supply the delivered power and the other one has no energy storage device and uses the grid supply during the compensation period. Here, closed-loop control is used for this topology of DVR [10] as it is shown in Fig. 1.

Fig. 1: Close loop control of Z-source inverter based DVR.

Here current mode close loop control is used to determine the appropriate value of shoot-through time (D_s). Current loop control can get a higher speed response by comparing the instantaneous inductor current and the reference current signal. Reference current signal is operated by passing the error signal of capacitor voltage through the PI controller. Reference signals for the DVR are calculated from the ideal supply reference voltage and the actual state of the supply voltage. Then these signals are turned to $dq0$. The error signal, between DVR reference voltage and the actual voltage of the DVR is minimized using PI controllers. This signals, generate $dq0$ signals to DVR, then transform to the three phase stationary reference frames which are in turn PWM modulated.

2.1. System with no Energy Storage

In this type, the requested energy, came from the grid supply by a shunt converter and will charge the DC-link capacitor to the actual state of the supply voltage. Based on the location of connecting the shunt converter to the grid supply, two topologies are considered for this type of system. Source side connected shunt converter and load side connected shunt converter, the second one is the best topology according to [8] and section 3 that explained the vantage of this topology for this operation. So here load side connected shunt converter topology of Z-source inverter based DVR is used for voltage harmonic compensation.

2.2. Load Side Connected Shunt Converter

As it is shown in Fig. 2, shunt converter is connected to the load side of the grid. The input voltage to the shunt converter is controlled and the DC-link voltage can be held constant by injecting sufficient voltage. This topology has the disadvantage of larger currents to be handled by the series converter than another topology.

Fig. 2: Load side connected shunt converter topology.

3. Compensation Strategy DVR

Load compensation could be done through active or reactive power injection by DVR. There are three compensation techniques based on using active, reactive, or both power by DVR. These methods are recognized as pre-fault compensation method, in-phase compensation method, and energy optimized compensation method. These strategies are introduced in this section followed by derivation of their respective equations. Some simulations would show the characteristics of each method individually [11], [12].

3.1. Pre-Fault Compensation Method

This method is mainly used for loads that are sensitive to phase jump such as thyristor controlled drives. In other word, both magnitude and phase of the load voltage are compensated in this strategy such that the load voltage during disturbances is as same as the one before disturbances. Fig. 3 shows this kind of compensation in a per-unit plane.
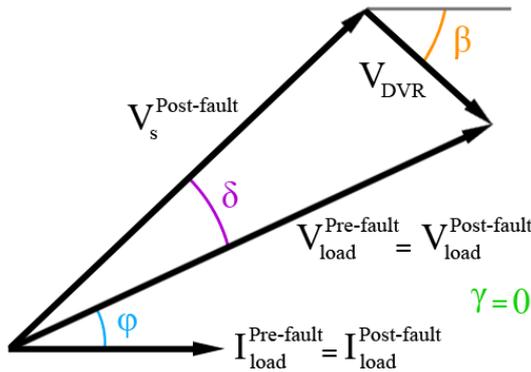
Fig. 3: Pre-fault compensation strategy.

In Fig. 3, $I_{load}^{Pre-fault} = 1\angle 0$ is the load current before disturbance that is considered as the reference vector. The load is selected as a general type so the load voltage could be defined as $I_{load}^{Pre-fault} = 1\angle\varphi$. The disturbance might change the source voltage magnitude from 1 to k with δ degree phase jump. Therefore the source voltage after disturbance can be defined as $V_s^{Pre-fault} = k\angle(\varphi + \delta)$. DVR should inject a voltage with appropriate magnitude and phase to compensate this disturbance. The DVR injected voltage is defined as $V_{DVR} = x\angle\beta$. Also the load voltage and current after compensation are the same as their values before disturbance which means $V_{load}^{Post-fault} = V_{load}^{Pre-fault}$ and $I_{load}^{Post-fault} = I_{load}^{Pre-fault}$. Moreover the resultant phase jump between load voltage before and after disturbance, γ, is zero in this compensating method. By these definitions, the DVR injected voltage can be calculated as follows:

$$V_{DVR} = V_{load}^{Post-fault} - V_s^{Post-fault} \Rightarrow$$

$$V_{DVR} = 1\angle\varphi - k\angle(\varphi + \delta) \Rightarrow$$

$$V_{DVR} = [\cos(\varphi) - k\cos(\varphi + \delta)] +$$
$$j[\sin(\varphi) - k\sin(\varphi + \delta)] \Rightarrow$$

$$x = \sqrt{1 + k^2 - 2k\cos(\delta)} \qquad (1)$$

$$\beta = \tan^{-1}\left(\frac{\sin(\varphi) - k\sin(\varphi + \delta))}{\cos(\varphi) - k\cos(\varphi + \delta)}\right). \qquad (2)$$

Equation (1) shows that the magnitude of the injected voltage only depends on the degree of distortion in the input voltage waveform. Fig. 4 shows this parameter versus the magnitude of the input voltage for different values of δ.
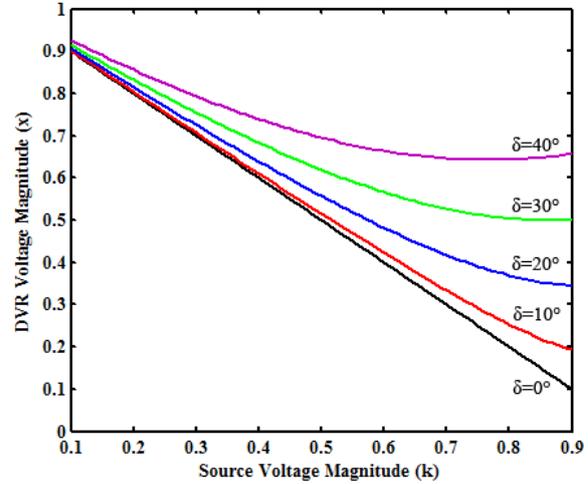
Fig. 4: Pre-fault compensation strategy: the magnitude of the injected voltage versus the magnitude of the source voltage.

3.2. In-Phase Compensation Method

In this method, DVR only compensates the load voltage magnitude so the phase jump would be remained uncompensated. Fig. 5 shows this control strategy. It is obvious that there is a phase difference between the load voltages before and after compensation. By using the same definitions in the previous section, the DVR injected voltage is as follows:

$$V_{DVR} = 1\angle(\varphi + \delta) - k\angle(\varphi + \delta) =$$

$$(1 - k)\angle(\varphi + \delta) \Rightarrow$$

$$x = 1 - k. \qquad (3)$$

$$\beta = \varphi + \delta. \qquad (4)$$

Therefore the load voltage after compensation can be written as $V_{load}^{Post-fault} = 1\angle(\varphi + \delta)$, so that the load current would be $I_{load}^{Post-fault} = 1\angle\delta$. Moreover there is a phase jump equal to $\gamma = \delta$ in the load voltage. The magnitude of the injected voltage for any disturbance's phase jump and any load power factor is shown in Fig. 5 that satisfies Eq. (3).
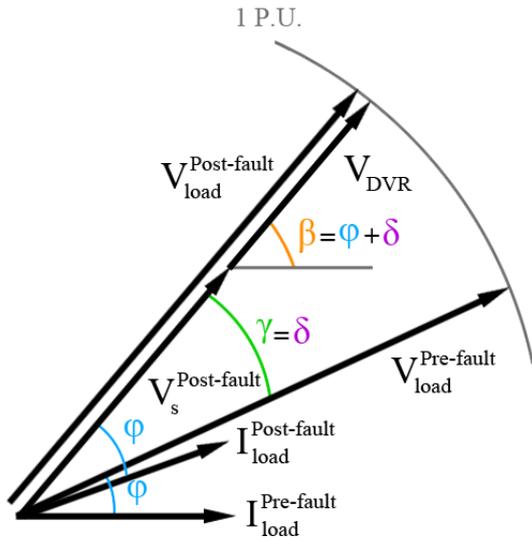
Fig. 5: In-phase compensation strategy.
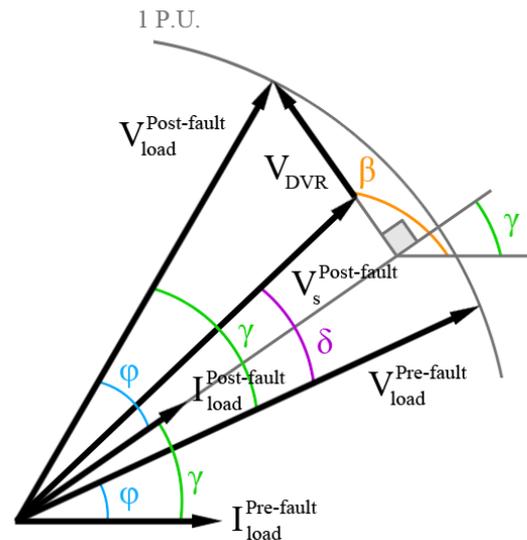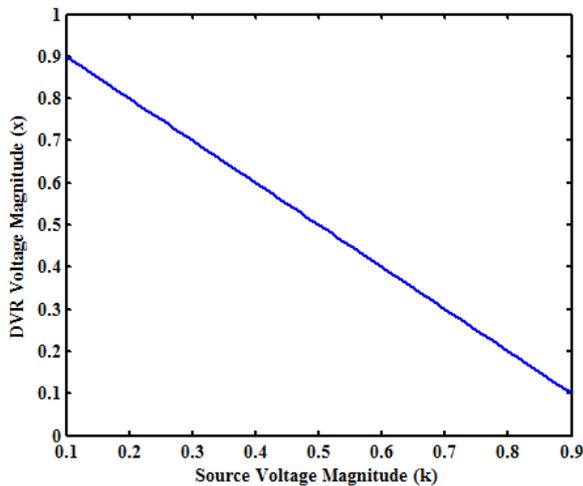
Fig. 6: In-phase compensation strategy: the magnitude of the injected voltage versus the magnitude of the source voltage.

3.3. Energy Optimized Compensation Method

It should be noticed that both previous strategies need a storage system to operate. However in energy optimized method, the capacity of this storage system is minimized. Furthermore in shallow sags, the compensation could be done only with reactive power and the amount of active power injection is zero. This strategy is based on injecting voltage in such a way that the injected voltage vector would be at almost 90 ° to the resultant load current vector. This will minimize the injection of active power and even it may be zero. Fig. 7 shows the basics of this strategy.

With the similar definitions like previous sections for voltage and currents, the injected voltage can be cal-

Fig. 7: Energy optimized compensation strategy.

culated as follows:

$$V_{DVR} = V_{load}^{Post-fault} - V_s^{Post-fault} \Rightarrow$$

$$V_{DVR} = 1\angle(\varphi + \gamma) - k\angle(\varphi + \delta) \Rightarrow$$

$$V_{DVR} = [\cos(\varphi + \gamma) - k\cos(\varphi + \delta)] +$$
$$j[\sin(\varphi + \gamma) - k\sin(\varphi + \delta)] \Rightarrow$$

$$x = \sqrt{1 + k^2 - 2k\cos(\delta - \gamma)}. \tag{5}$$

$$\beta = \tan^{-1}\left(\frac{\sin(\varphi + \gamma) - k\sin(\varphi + \delta)}{\cos(\varphi + \gamma) - k\cos(\varphi + \delta)}\right). \tag{6}$$

According to Fig. 8 the injection voltage phase angle is $\beta = \pi/2 + \gamma$. By replacing this value in Eq. (6), the load phase jump can be calculated after some manipulations:

$$\tan^{-1}\left(\frac{\sin(\varphi + \gamma) - k\sin(\varphi + \delta)}{\cos(\varphi + \gamma) - k\cos(\varphi + \delta)}\right) = \frac{\pi}{2} + \gamma \Rightarrow$$

$$\frac{\sin(\varphi + \gamma) - k\sin(\varphi + \delta)}{\cos(\varphi + \gamma) - k\cos(\varphi + \delta)} = -\cot\gamma \Rightarrow$$

$$\gamma = \varphi + \delta - \cos^{-1}\left(\frac{1}{k}\cos(\varphi)\right). \tag{7}$$

To ensure that Eq. (7) is feasible, $\frac{1}{k}\cos(\varphi) \le 1$ has to be established. So the source amplitude must be more than the load power factor or $k \ge \cos(\varphi)$. If this situation is not yielded, γ should be calculated through Eq. (8):

$$\gamma = \varphi + \delta. \tag{8}$$

Figure 8 and Fig. 9 show the load phase jump and the injected voltage magnitude for different values of δ. The load power factor is chosen as 0,7.
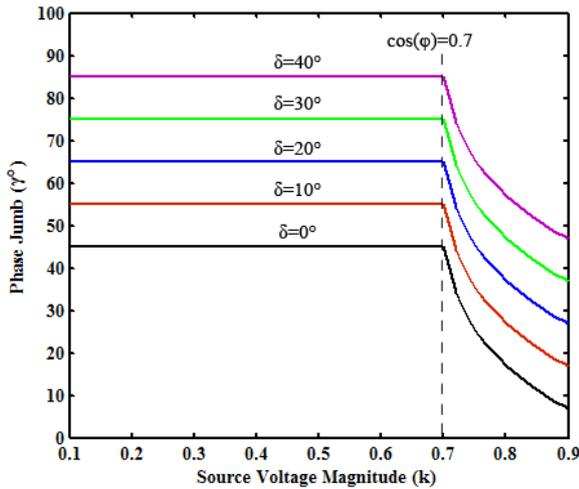
Fig. 8: Energy optimized compensation strategy: the phase jump of the load voltage versus the magnitude of the source voltage for $PF = 0,7$.

Fig. 9: Energy optimized compensation strategy: the magnitude of the injected voltage versus the magnitude of the source voltage for $PF = 0,7$.
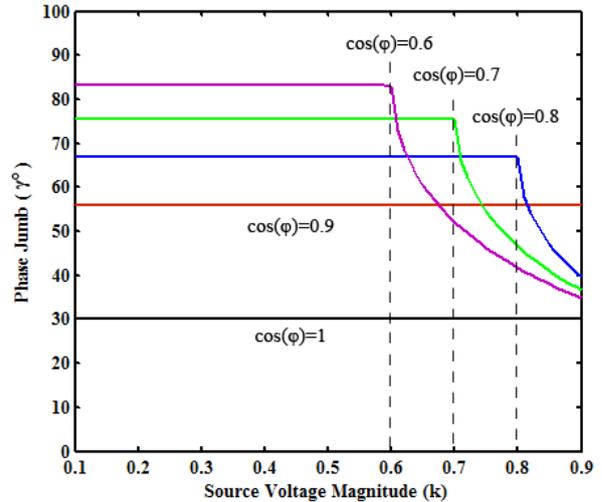
Fig. 10: Energy optimized compensation strategy: the phase jump of the load voltage versus the magnitude of the source voltage for $\delta = 30$ °.

Fig. 11: Energy optimized compensation strategy: the magnitude of the injected voltage versus the magnitude of the source voltage for $\delta = 30$ °.

4. Analysis of the Input Source Current

According to Fig. 12, the Z-source inverter based DVR has no energy storage and the required power for compensation is taken from the grid itself. So the source current can be a comparative characteristic of different compensation techniques for this kind of DVR.

As it has been mentioned, Z-source converter is able to control its input power factor. The shunt converter input voltage is the load voltage which is $V_{load}^{Post-fault} = 1\angle(\varphi + \gamma)$ after compensation. By considering a unity power factor for the input of Z-source converter, the current of shunt converter would
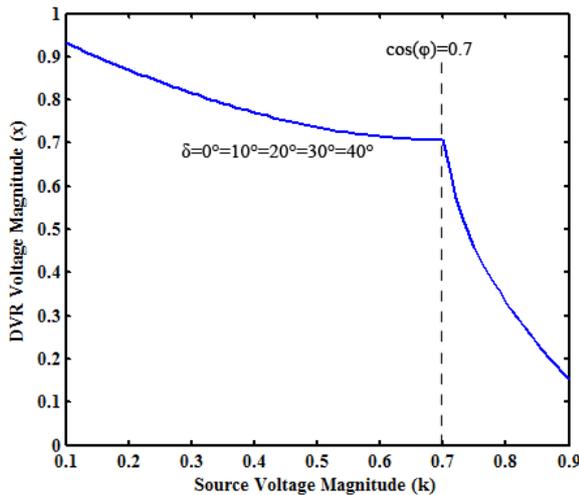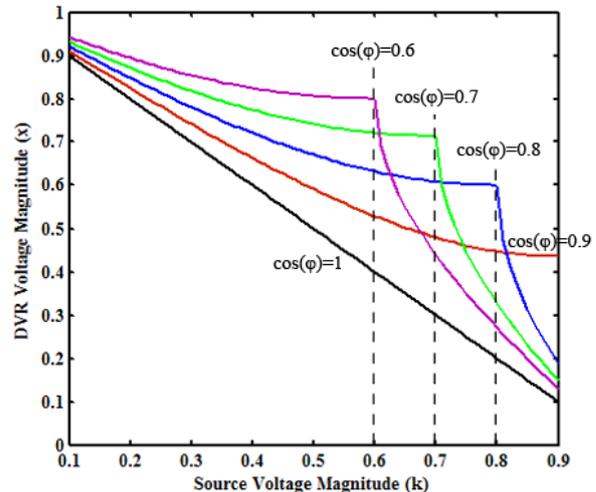
In Fig. 10 and Fig. 11, $\delta = 30$ ° is constant and the load phase jump and the injected voltage magnitude are plotted for different load power factor. There are some notices in these figures. It should be noted that the injected voltage magnitude is independent of δ. Moreover the break-points in these figures are relevant to the load power factor. In other word, the load can be compensated only through the injection of reactive power for $k \geq \cos(\varphi)$; otherwise there would be an active power injection too.

Fig. 12: Schematics of a DVR based on Z-source inverter.

be $I_{MC}^{Post-fault} = y\angle(\varphi + \gamma)$. Also the source current is defined as $I_s^{Post-fault} = z\angle(\xi)$. Because there is no energy storage in the structure, the input and output active power of the Z-source converter (with shunt converter) should be equal. Therefore:

$$P_{MC1}^{Post-fault} = P_{MC2}^{Post-fault} \Rightarrow$$

$$\Re\left\{\left[V_{load}^{Post-fault}\right]\left[I_{MC}^{Post-fault}\right]^*\right\} =$$

$$\Re\left\{\left[\frac{1}{n}V_{DVR}\right]\left[nI_s^{Post-fault}\right]^*\right\} \Rightarrow$$

$$\Re\left\{[1\angle(\varphi + \gamma)]\left[y\angle(\varphi + \gamma)\right]^*\right\} =$$

$$\Re\left\{[x\angle\beta]\left[z\angle\xi\right]^*\right\} \Rightarrow$$

$$y = xz\cos(\xi - \beta), \qquad (9)$$

now by using KCL we have:

$$I_{load}^{Post-fault} = I_s^{Post-fault} - I_{MC}^{Post-fault} =$$

$$z\angle\xi - y\angle(\varphi + \gamma) \Rightarrow$$

$$1\angle\gamma = [z\cos(\xi) - y\cos(\varphi + \gamma)] +$$

$$j[z\sin(\xi) - y\sin(\varphi + \gamma)] \Rightarrow$$

$$\sqrt{z^2 + y^2 - 2zy\cos(\xi - \varphi - \gamma)} = 1, \qquad (10)$$

$$\tan^{-1}\left(\frac{z\sin(\xi) - y\sin(\varphi + \delta))}{z\cos(\xi) - z\cos(\varphi + \delta)}\right) = \gamma, \qquad (11)$$

after some manipulation, Eq. (11) yields to:

$$\sin(\xi - \gamma) = \frac{y\sin(\varphi + \gamma) - y\tan(\gamma)\cos(\varphi + \gamma)}{z\sqrt{1 + \tan^2(\gamma)}}, \qquad (12)$$

by inserting Eq. (9) in to Eq. (12) we have Eq. (13). And by inserting Eq. (9) in to Eq. (10) we have Eq. (14):

Equation (13) and Eq. (14) can be applied to all of the compensation strategies. It should be noted that for the pre-fault method $\gamma = 0$, for the in-phase method $\gamma = \delta$, and for the energy optimized method can be calculated by Eq. (7) or (8).

5. Comparison Between Compensation Strategies

In this section, all compensation strategies are compared with each other. There are different criteria for comparison. Suppose that a disturbance with $\delta = 45\,^\circ$ occurs and the load power factor is $\cos(\varphi) = 0,6$. In Fig. 13 to Fig. 15 the magnitude of the injected voltage, the phase jump of the load voltage, and the magnitude of the input source current are shown, respectively. It could be observed that:

- The in-phase method has the least injection voltage magnitude.

- For shallow disturbances, energy optimized method has less injection voltage magnitude than the pre-fault method.

- For large disturbances, the pre-fault compensation strategy has the most magnitude of the DVR injected voltage. This means that in this compensation method, DVR components should have a higher voltage rating compared with the other methods.

- The energy optimized method has the most load phase jump angle followed by the in-phase method. This parameter can be a criterion of the load voltage distortion especially at the start and the end of the disturbance occurring time.

- The pre-fault method compensates the load voltage to its pre-fault value so it makes no phase jump in the load voltage.

- The energy optimized method and the pre-fault method have the most and the least magnitude of the input current, respectively. The higher value of the input current makes a more severe disturbance for the upstream loads because it makes more voltage drop. Moreover the DVR components should have a higher current rating.

6. Simulation

Load side connected Shunt converter topology of Z-source inverter based DVR that operate based on pre-fault, in phase and energy optimized compensation methods are simulated in MATLAB/ SIMULINK to study the results of simulation tests. Table 1 shows the characteristic of Z-source inverter, DC-link and also load parameters. The injection transformer ratio is one. Phase a and c are stricken to the same fault that cause to reduce the peak voltage from 300 V to 120 V and 32 $^\circ$ shift phase also phase b is stricken to

$$\xi = \tan^{-1} \left(\frac{\sin(\gamma)\sqrt{1 + \tan^2(\gamma)} + x\cos(\beta)\left[\sin(\varphi + \gamma) - \tan(\gamma)\cos(\varphi + \gamma)\right]}{\cos(\gamma)\sqrt{1 + \tan^2(\gamma)} + x\sin(\beta)\left[\sin(\varphi + \gamma) - \tan(\gamma)\cos(\varphi + \gamma)\right]} \right). \tag{13}$$

$$z = \frac{1}{\sqrt{1 + x^2\cos^2(\xi - \beta) - 2x\cos(\xi - \beta)\cos(\xi - \varphi - \gamma)}}. \tag{14}$$
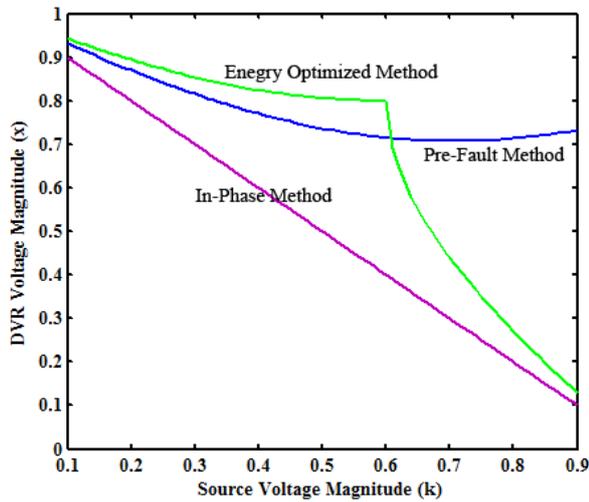
Fig. 13: Comparison between different control strategies: the magnitude of the injected voltage versus the magnitude of the source voltage.
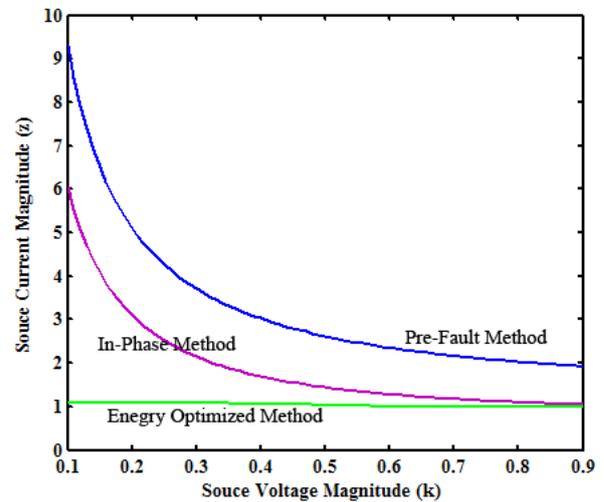
Fig. 15: Comparison between different control strategies: the magnitude of the input source current versus the magnitude of the source voltage.

Tab. 1: Characteristic of grid, load and converter.

	Parameters	Values
Grid	Grid phase voltage	215 V
	Frequency	50 Hz
	Source resistance	1 mΩ
	Source inductance	1 µH
Load	Load resistance	50 Ω
	Load inductance	200 µH
DVR	Ratio of transformer	1:1
	Output filter inductance	10 mH
	Output filter capacitance	400 µF
	Inductance of network	450 µH
	Capacitance of netowrk	470 µF
	Switching frequency	10 kHz
Link-DC	DC voltage	20 V
	Capacitance	5 mF

Fig. 14: Comparison between different control strategies: the phase jump of the load voltage versus the magnitude of the source voltage.

6.1. Pre-Fault Compensation Method Study

Figure 17 b), d) shows the effectiveness of theproposed topology whenthe pre-fault method is used to compensate the occurred fault. As mentioned before, this method injects the voltage to compensate not only the reduction in amplitude but also thephase jump of the load voltage. According to Tab. 2 the injected voltage has a peak value of about 217 V with the angle of $-16\,^\circ$ for phase a and c, and 275 V with the angle of $-17\,^\circ$ for phase b. The load voltage is almost close to $300\angle0$. This method has one or two cycles delay creating these

the different fault that causes to reduce the amplitude of voltage to 81 V and 54 $^\circ$ shift phase. Fig. 16 a), b) describes this image fault.

a)

b)
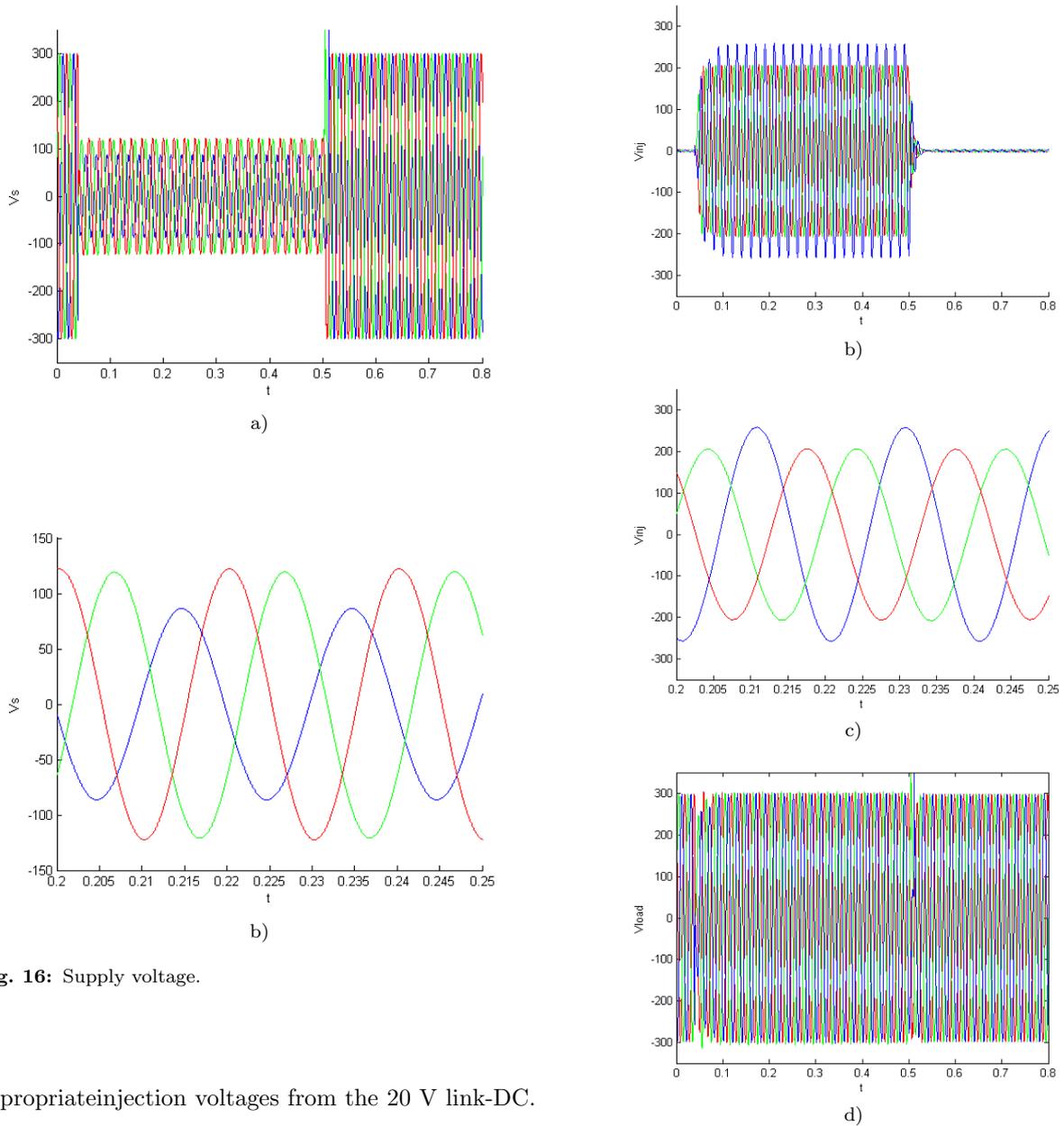
Fig. 16: Supply voltage.

appropriateinjection voltages from the 20 V link-DC.

a)

b)

c)

d)

e)
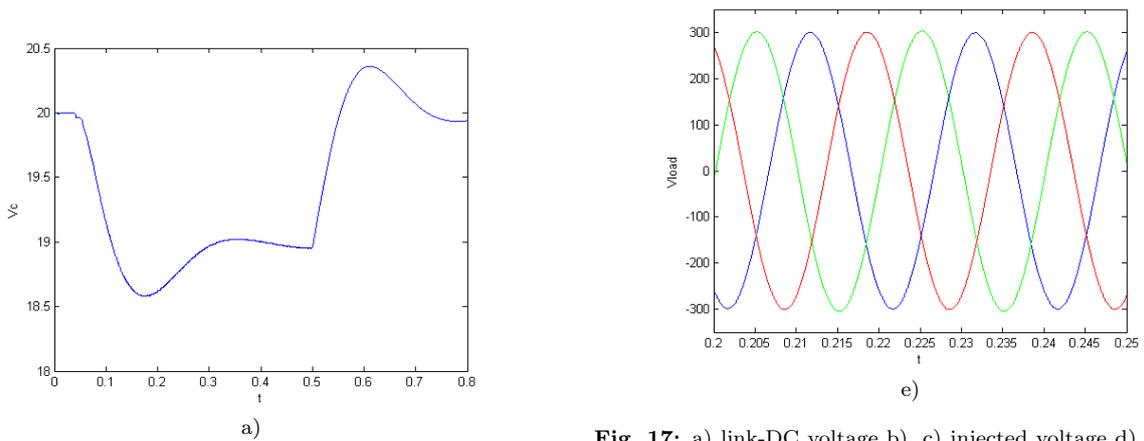
Fig. 17: a) link-DC voltage b), c) injected voltage d), e) compensated voltage.

6.2. In-Phase Compensation Method Study

Figure 18 b), d) shows the effectiveness of thementioned topology usingthe in-phase method as its compensation strategy. As previously said, this method compensatesjust the amplitude of the voltage and the phase jump remains in the load voltage after compensation. According to Tab. 2 the injected voltage has a peak value of 178 V withthe angle of 31 ° for phase a and c, and 217 V withthe angle of 55 ° for phase b. So the injected voltage is almost in-phase with the supply voltage. It is expected thatthis method has the least amplitude of the injected voltage compared with other strategies. Moreover, its delay time is about half a cycle. The injection voltage from the 20 V link-DC makes the load voltage amplutide increasing to about 300 V but the phase jump is not compensated.
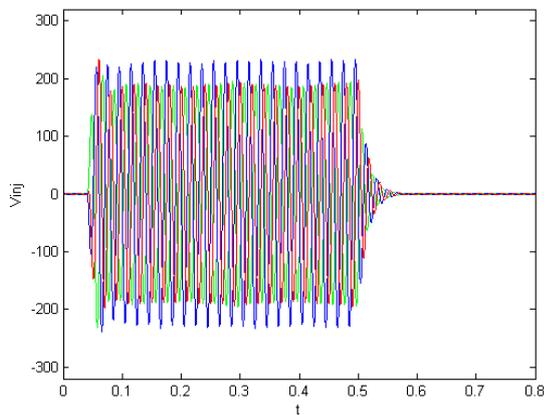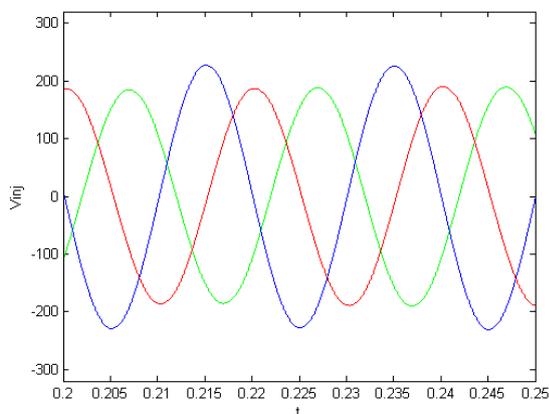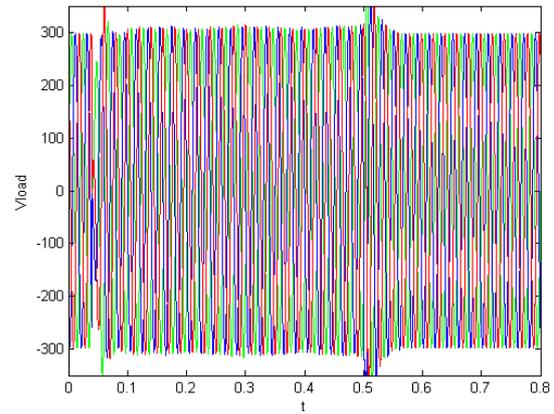
c)
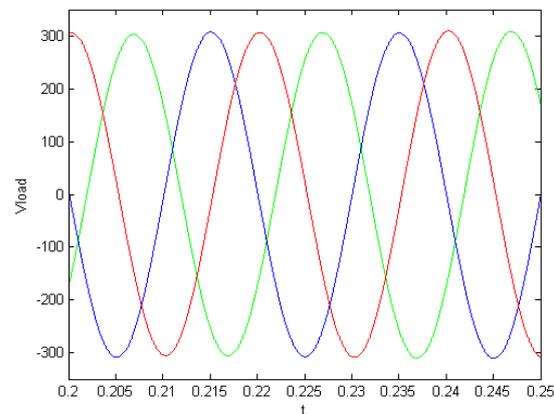
d)

Fig. 18: a), b) injected voltage c), d) compensated voltage.

a)

b)

6.3. Energy Optimized Compensation Method Study

Figure 19 a), b) shows the load current during the fault. There is 33 ° phase jump for phase a and c whilea 60 ° phase jump occuredat phase b. Therefore the injected voltage angle should be about 120 ° for phase a and c, and 150 ° for phase b. The effectiveness of this compensation method is shown in Fig. 19 c), e). As mentioned before, this method injects the voltage whereas the minimum energy is consumed in comparison with other methods. According to Tab. 2 the injected voltage has a peak value of about 265 V with the angle of 117 ° for phase a and c. The amplitude and angle of the injected voltage of phase b are 300 V and 152 °, respectively. It is obvious that this method requires the most voltage amplitude to compesate the occured fault. It needs around two or three cycles to create the injection voltage from the 20 V DC-link. The compensated load voltage has a peak valueof about 300 V for all phases, the angle of 93 ° for phase a and c, and the angle of 135 ° for phase b.

a)

b)

c)

d)

e)

f)
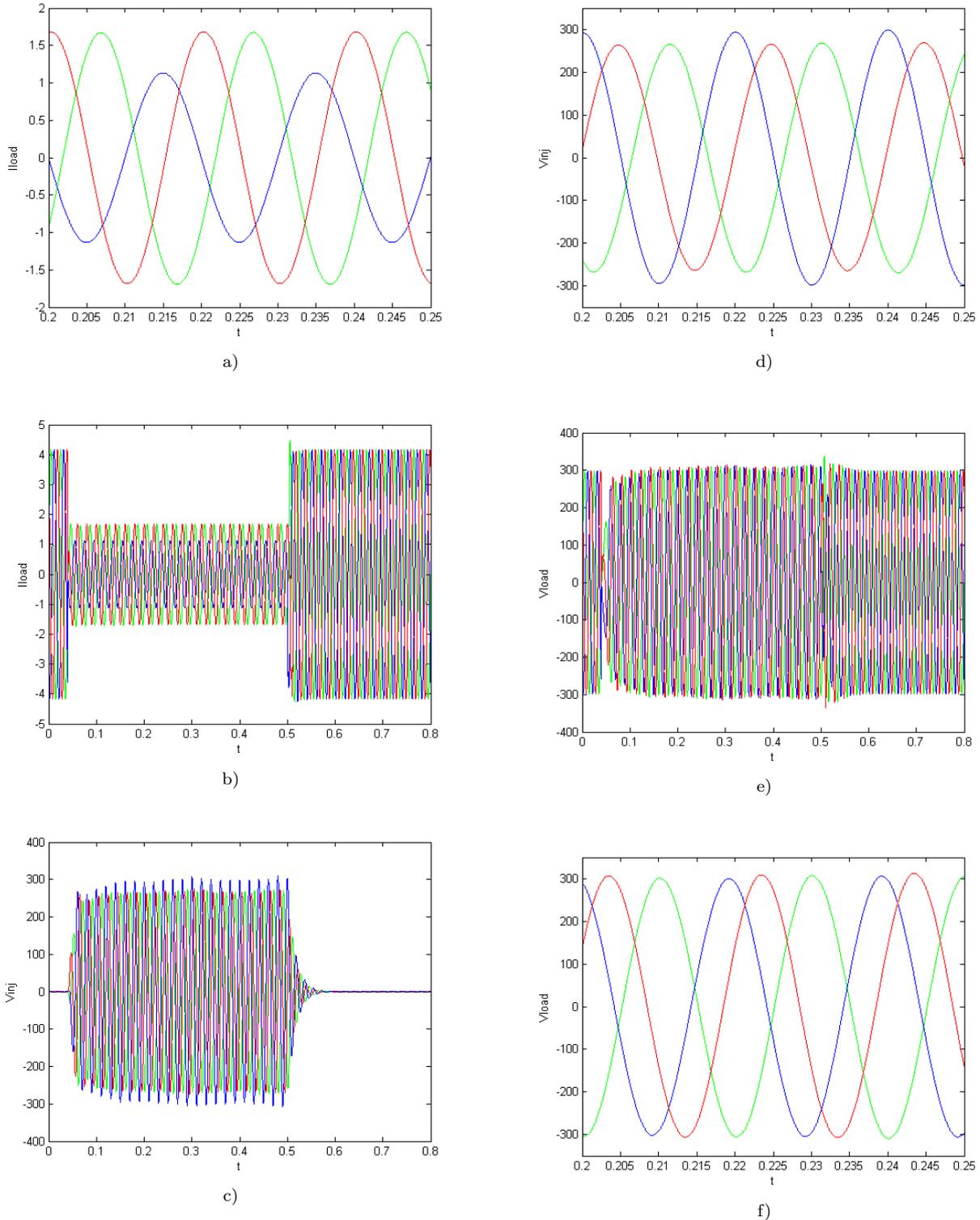
Fig. 19: a), b) load current c), d) injected voltage e), f) compensated voltage.

7. Conclusion

Load side connected shunt converter topology is the best topology of DVR according to [8] that used VSI as a series converter. In this paper, Load side connected shunt converter topology of DVR with Z-source inverter as a series converter is used. In this paper different compensation strategies to provide the injec-

tion voltage for a Z-source converter based DVR are analyzed. Different comparison criteria are studied. Results show that if the load is sensitive to voltage phase jump, pre-fault method should be used. However this method draws more current from the source which

needs DVR components with higher current rating. If the load is insensitive to phase jump either in-phase or energy optimized methods can be used to compensate it. Here pre-fault compensation method is used for the identified topology of DVR. Simulation results show the benefit of this compensation method for this topology of Z-source inverter based DVR. The in-phase method has the least injection voltage magnitude that makes the components cheaper. Moreover for a similar disturbance compensation, the in-phase strategy needs less transformer voltage ratio compared to other methods. The energy optimized method needs the least input current magnitude to compensate disturbances. This will create less voltage drop for upstream loads and also the possibility to design a DVR with less current rating components.

Tab. 2: Simulation results.

Phase		Amplitude [V]			Phase [°]		
		A	**B**	**C**	**A**	**B**	**C**
Pre-fault compensation method	V_s	120	81	217	32	54	32
	V_{inj}	217	275	217	-16	-17	-16
	V_{load}	303	302	303	4	2	4
In phase compensation method	V_s	120	81	217	32	54	32
	V_{inj}	178	217	178	31	55	31
	V_{load}	297	299	297	31	54	31
Energy opt. compensation method	V_s	120	81	217	32	54	32
	V_{inj}	265	300	265	117	152	117
	V_{load}	303	305	303	93	135	93

References

[1] AL-OTHMAN, A. K. and T. H. ABDEL-HAMID. Elimination of harmonics in multilevel inverters with non-equal dc sources using PSO. *Energy Conversion and Management*. 2009, vol. 50, iss. 3, pp. 756–764. ISSN 0196-8904. DOI: 10.1016/j.enconman.2008.09.047.

[2] NGUYEN, M.-K., Y.-G. JUNG and Y.-C. LIM. Single-phase Z-source voltage sag/swell compensator. In: *IEEE International Symposium on Industrial Electronics*. Seoul: IEEE, 2009, pp. 24–28. ISBN 978-1-4244-4347-5. DOI: 10.1109/ISIE.2009.5217933.

[3] VILATHGAMUWA, D. M., C. J. GAJANAYAKE, P. C. LOH and Y. W. LI. Voltage sag compensation with Z-source inverter based Dynamic Voltage Restorer. In: *Industry Applications Conference, 2006. 41st IAS Annual Meeting*. Tampa: IEEE, 2006, pp. 2242–2248. ISBN 1-4244-0364-2. DOI: 10.1109/IAS.2006.256854.

[4] RAJAKARUNA, S. and L. JAYAWICKRAMA. Steady-State analysis and designing impedance network of Z-Source Inverters. *IEEE Transactions on Industrial Electronics*. 2010,

vol. 57, iss. 7, pp. 2483–2491. ISSN 0278-0046. DOI: 10.1109/TIE.2010.2047990.

[5] VINNIKOV, D. and I. ROASTO. Quasi-Z-source-based isolated DC/DC converters for distributed power generation. *IEEE Transaction on Industrial Electronics*. 2011, vol. 58, iss. 1, pp. 192–201. ISSN 0278-0046. DOI: 10.1109/TIE.2009.2039460.

[6] VINNIKOV, D., I. ROASTO, R STERZELECKI and M ADAMOWICZ. Step-up DC/DC converters with cascaded Quasi-Z-source network. *IEEE Transaction on Industrial Electronics*. 2012, vol. 59, iss. 10, pp. 3727–3736. ISSN 0278-0046. DOI: 10.1109/TIE.2011.2178211.

[7] PENG, F. Z. Z-source inverter. *IEEE Transaction on Industry Applications*. 2003, vol. 39, iss. 2, pp. 504–510. ISSN 0093-9994. DOI: 10.1109/TIA.2003.808920.

[8] NIELSEN, J. G. and F. BLAABJERG. A detailed comparison of system topologies for dynamic voltage restorers. *IEEE Transaction on Industrial Applications*. 2005, vol. 41, iss. 5, pp. 1272–1280. ISSN 0093-9994. DOI: 10.1109/TIA.2005.855045.

[9] NIELSEN, J. G., M. NEWMAN, H. NIELSEN and F. BLAABJERG. Control and testing of a dynamic voltage restorer (DVR) at medium voltage level. *IEEE Transactions on Power Electronics*. 2004, vol. 19, iss. 3, pp. 806–813. ISSN 0885-8993. DOI: 10.1109/TPEL.2004.826504.

[10] GAJANAYAKE C. J., D. M. VILATHGAMUWA and P. C. LOH. Development of a comprehensive model and a multiloop controller for z-source inverter DG systems. *IEEE Transaction on Industrial Electronics*. 2007, vol. 54, iss. 4, pp. 2352–2359. ISSN 0278-0046. DOI: 10.1109/TIE.2007.894772.

[11] RAMACHANDARAMORTHY, V. K., C. FITZER, A. ARULAMPALAM, C. ZHAN, M. BARNES and N. JENKINS. Control of a battery supported dynamic voltage restorer. *IEE Proceedings - Generation, Transmission and Distribution*. 2002, vol. 149, iss. 5, pp. 533–542. ISSN 1350-2360. DOI: 10.1049/ip-gtd:20320658.

[12] BANAEI, M. R., S. H. HOSSEINI, S. KHANMOHAMADI and G. B. GHAREHPETIAN. Verification of a new control strategy for a dynamic voltage restorer by simulation. *Simulation modeling practice and theory*. 2006, vol. 14, iss. 2. pp. 112–125. ISSN 1569-190X. DOI: 10.1016/j.simpat.2005.03.001.

About Authors

Abolfazl KAZEMDEHDASHTI was born in Tehran, Iran, on 28 April 1987. He received the B.Sc. degree in Electrical Engineering from the Chamran University of Ahvaz, Ahvaz, Iran in 2010. He is currently a M.Sc. student of Electrical Engineering in Shiraz University, Shiraz, Iran. His research interests include power converters, power quality, and distributed generation.

Ali Reza SEIFI was born in Shiraz, Iran, on August 9, 1968. He received his B.Sc. degree in Electrical Engineering from Shiraz University, Shiraz, Iran, in 1991, and M.Sc. degree in Electrical Engineering from The University of Tabriz, Tabriz, Iran, in 1993, and Ph.D. degree in Electrical Engineering from Tarbiat Modarres University (T.M.U), Tehran, Iran, in 2001, respectively.

He is currently as an Associate professor in Department of Power and Control Eng, School of Electrical and Computer Engineering, Shiraz University, Shiraz, Iran. His research areas of research interest are Power plant simulation, Power systems, Electrical machines simulation, Power electronic and Fuzzy optimization.

Amin Shabanpour HAGHIGHI was born in Shiraz, Iran, on July 27, 1986. He received the B.Sc. and M.Sc. degrees in Electrical Engineering from Shiraz University, Shiraz, Iran in 2008 and 2011, respectively. He is currently pursuing the Ph.D. degree in Electrical Engineering at Shiraz University, Shiraz, Iran. His research interests are Power electronics, power quality analysis, and FACTS devices.